

Unexpected side reactions dominate the oxidative transformation of aromatic amines in the Co(II)/peracetic acid system

Jing-Hang Wu ^a, Tian-Hao Yang^a, Fei Chen ^{a,*} and Han-Qing Yu ^{a,*}

^aDepartment of Environmental Science and Engineering, CAS Key Laboratory of Urban Pollutant Conversion, University of Science and Technology of China, Hefei 230026, China

*To whom correspondence should be addressed: Email: fchen05@ustc.edu.cn (F.C.); Email: hqyu@ustc.edu.cn (H.-Q.Y.)

Edited By: Levi Thompson

Abstract

Aromatic amines (AAs), ubiquitous in industrial applications, pose significant environmental hazards due to their resistance to conventional wastewater treatments. Peracetic acid (PAA)-based advanced oxidation processes (AOPs) have been proposed as effective strategies for addressing persistent AA contaminants. While the organic radicals generated in these systems are believed to be selective and highly oxidative, acetate residue complicates the evaluation of AA removal efficiency. In this work, we explored transformation pathways of AAs in a representative Co(II)-catalyzed PAA system, revealing five side reactions (i.e. nitrosation, nitration, coupling, dimerization, and acetylation) that yield 17 predominantly stable and toxic by-products. The dominant reactive species was demonstrated as Co–OOC(O)CH₃, which hardly facilitated ring-opening reactions. Our findings highlight the potential risks associated with PAA-based AOPs for AA degradation and provide insights into selecting suitable catalytic systems aimed at efficient and by-product-free degradation of pollutants containing aromatic –NH₂.

Keywords: peracetic acid, aromatic amines, toxic by-products, Co–OOC(O)CH₃ complex, oxidative coupling

Significance Statement

Catalytic oxidation processes are widely applied for wastewater treatment. Yet, the unforeseen risks caused by the unexpected side reactions have remained largely unexplored. Here, we reveal the formation of notably toxic and persistent by-products in treating various aromatic amines using an emergent Co(II)/peracetic acid system. By examining the pathways of these side reactions, we unveil the universal formation of unexpected by-products. Furthermore, this study paves the way for exploring the responsible reactive species for side reactions and offers new insights for designing more safe and efficient catalytic oxidation systems.

Introduction

Aromatic amines (AAs) are widely used in pharmaceuticals, agriculture, and various industries (1, 2). Due to their inherent toxicity and persistence in soil and water bodies, AAs pose significant risks to human health and the environment (3). Advanced oxidation processes (AOPs) have been applied as a solution to treat wastewater contaminated with ecotoxic AAs. However, the conventional Fenton process and the developed H₂O₂-based AOPs demonstrate limited oxidizing capabilities. Thus, highly oxidative radicals, such as sulfate radicals (SO₄^{•−}), iodate radicals (IO₃[•]), and organic radicals (CH₃C(O)OO[•] and CH₃C(O)O[•]), are generated by activating different oxidants to effectively degrade chemically stable contaminants (4–6). Notably, organic radicals derived from peracetic acid (PAA) have been identified as a strong oxidant for removing sulfa drugs (7–10). Also, PAA has exhibited a similar

oxidizing performance to peroxymonosulfate (PMS) in various water treatment scenarios (11, 12). Moreover, its residual product, acetate, is relatively harmless and poses minimal environmental risk.

However, the reactive nature of the aromatic amino moiety (–NH₂) makes it highly susceptible to oxidation, leading to the formation of unexpected by-products in the oxidative degradation of AAs (13, 14). The generation of nitrosation and nitration products has been identified as a critical factor contributing to the risks associated with the use of AOPs (15). Besides, compounds featuring azo bonds (–N=N–) are frequently detected in oxidative reactions, constituting highly toxic, carcinogenic, and mutagenic products (16). The electron-deficient characteristics of these azo compounds render them resistant to conventional aerobic biological treatments, exacerbating the environmental risks of AA removal using AOPs (17). Therefore, an effective AOP system should be

Competing Interest: The authors declare no competing interest.

Received: July 24, 2023. **Accepted:** January 22, 2024

© The Author(s) 2024. Published by Oxford University Press on behalf of National Academy of Sciences. This is an Open Access article distributed under the terms of the Creative Commons Attribution-NonCommercial-NoDerivs licence (<https://creativecommons.org/licenses/by-nc-nd/4.0/>), which permits non-commercial reproduction and distribution of the work, in any medium, provided the original work is not altered or transformed in any way, and that the work is properly cited. For commercial re-use, please contact journals.permissions@oup.com

capable of attacking the main chains of targeted pollutants, resulting in chain leakage and ring-opening products (18).

Recently, when treating contaminants with $-NH_2$ moiety, various toxicity-enhancing by-products, such as azo compounds and nitro(so) by-products, have been detected in different AOPs (18–21). Partial mineralization and unexpected oxidation of amines have also been recognized in other oxidation processes (22). However, the use of PAA as an oxidant could significantly increase the total organic carbon and chemical oxygen demand of the final effluent. While the substantial amount of residual organics may facilitate subsequent biological treatment, it hinders the necessary evaluation of the actual mineralization of organic pollutants (23). Thus, although chemically stable by-products have commonly been detected in PAA-based AOPs (7–9, 24, 25), the risks are further whitewashed. Hence, investigating the prevalence and intrinsic patterns of side reactions, pathways of $-NH_2$ transformation, and the effects of substituents on preferences is crucial for treating AA-containing wastewater using catalytic oxidation strategies.

In this work, we investigated the side reactions of AAs in the Co(II)/PAA system with a focus on their universality and diversity. We compared the different transformation pathways of these reactions in detail and examined the effects of the substituents on the propensity for the side reactions. Furthermore, we identified the responsible reactive species for the unexpected oxidation of aromatic $-NH_2$. The results from this work could serve as an important guide for the application of PAA-activated systems for the treatment of AA-containing wastewater.

Results and discussion

Transformations of sulfonamides in the Co(II)/PAA system

To gain insight into the transformation pathways of sulfonamides in the typical Co(II)/PAA system, we investigated the degradation of three representative sulfa drugs, including sulfamethoxazole (SMZ), sulfadiazine (SD), and sulfamerazine (SMR). The intermediate products were identified (Fig. 1), revealing similar fates of all three sulfonamides during oxidation. The decrease in sulfa concentration might be attributed mainly to $-NH_2$ oxidations, including nitrosation, nitration, and N-coupling. However, no further degradation of these by-products was observed.

We predicted the potential toxicities of the identified by-products generated in the Co(II)/PAA/sulfa systems using the ECOSAR program (Table S3). The obtained results show that the three initial sulfas exhibited toxicity toward daphnids and could induce severe chronic effects on the three organisms (i.e. fish, daphnia, and green algae). However, in the Co(II)/PAA system, advanced oxidation of sulfas formed potentially “very toxic” N-coupling by-products, such as **A**-SMZ with a ChV value of 0.520 mg L^{-1} and **OOA**-SMR with a ChV value of 0.669 mg L^{-1} , as determined by chronic toxicity analysis. Although the PAA-based AOPs have been commonly recognized as effective treatment methods for sulfas, their inefficient sulfonamide cleavage and the generation of harmful intermediates or by-products will greatly hinder their practical applications. This phenomenon is neglected in previous studies, and there is a lack of toxicity assessment and mineralization of subsequent by-products with a single removal efficiency guarantee.

In general, the oxidation of $-NH_2$ to $-NO$ and $-NO_2$ would not remarkably affect the toxicity of sulfas. However, hydroxylation would increase their chronic toxicities. The oxidative coupling of $-NH_2$ led to the formation of azo by-products, that were not produced in biodegradation (26), and generally exhibited higher

toxicities than the parent sulfas. Moreover, the breakage of the S–N bond in the sulfonamide group resulted in the formation of less toxic **C1**-products (**C1**-SMZ, **C1**-SD, and **C1**-SMR). Conversely, the cleavage of the sulfo-group ($-SO_3H$) resulted in the formation of highly toxic **C2**-products. In summation, the majority of the unforeseen side reactions were attributed to the oxidative conversion of the aromatic $-NH_2$. Consequently, it is imperative to thoroughly investigate the oxidation mechanism and preferences associated with these transformations.

Transformations of aniline in the Co(II)/PAA system

To further explore the reactions of aromatic $-NH_2$ under the oxidative condition in the Co(II)/PAA system, we examined the transformation of the simplest AA, aniline (Fig. 2a). The hydroxylation products of aromatic compounds are reported to be harmful or toxic to organisms, but could be effectively removed by HO^\bullet -dominated AOPs (27). However, no further oxidation products of aniline were found in the Co(II)/PAA system. Moreover, similar to the aforementioned sulfa degradation, the $-NH_2$ could be directly oxidized and thus transformed into various by-products. Notably, the hydroxylation products of azobenzene were detected. Such hydroxylation reactions might reduce the assessed concentration of azobenzene, while in fact the azo by-products were not destroyed, thus posing a potential risk.

Due to the complex side reactions and their competition, the effect of reactant dosage on the relative yields of different by-products showed complex characteristics. At low aniline dosages ($\leq 20 \text{ mg L}^{-1}$), the yield of hydroxylated products remained at a relatively high level, but neither azobenzene (**A**-aniline) nor 4-aminodiphenylamine (**D**-aniline) was detected (Fig. 2b). When the aniline concentration was increased, nitrobenzene (**X**-aniline) yield decreased, while the **A**- and **D**-product yields increased. This result indicates a cascade oxidative side reaction in the Co(II)/PAA/aniline system. The generation of the terminal $-NH_2$ -oxidation product, nitrobenzene, would be understandably suppressed when the oxidative active species were consumed in other side reactions. Also, the high concentration of aniline increased the probability of direct oxidative coupling and dimerization. The by-products observed in the Co(II)/PAA system were found to be stable and resistant to further degradation. In contrast, the yields of **Y**-, **X**-, **O**-, and **OA**-products remarkably increased with the increase in PAA dosage. Thus, the stable by-products were not a result of insufficient PAA, and the excess oxidant dose could not remove the formed long-lasting by-products (Fig. 2c). Both the $-NO$ and $-NO_2$ are strong electron-withdrawing groups, increasing the structural stability of the products and decreased the removal effectiveness (28). In addition, aromatic azo compounds have been reported to exhibit high chemical stability and cause severe environmental and health concerns (29).

When aniline was treated with the PAA-based system, the resulting solution exhibited a significant color change (Fig. S1). Due to a low catalyst dose and negligible spectral interference, the Co(II)/PAA system would be a reliable platform for kinetic studies based on UV–Vis spectra. Spectroscopic kinetics were acquired at 350 nm to indicate the generation of azobenzene chromophores. Similar to the interactions observed in the Co(II)/PAA system, the Co(II)/PMS, the Fe(II)/PAA, and the Ru(III)/PAA systems also continuously transformed aniline into azo by-products (Fig. 3a), suggesting the ubiquity of such a side reaction. The Co(II)/PMS system has been reported to efficiently degrade SMZ, and concurrently transform SMZ into $-NH_2$ -oxidation by-products

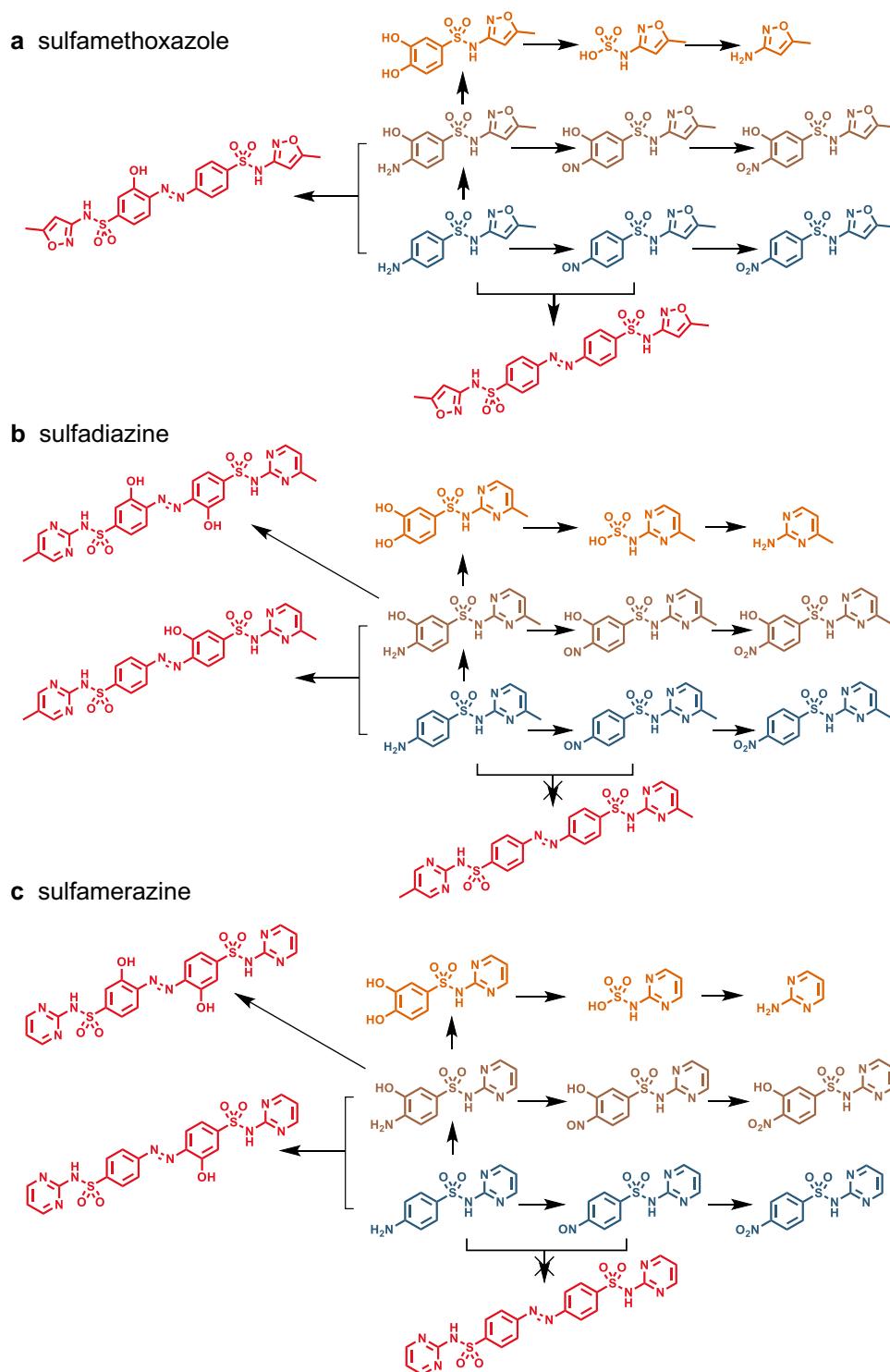


Fig. 1. Transformation pathways of sulfa drugs. a) SMZ, b) SD, and c) SMR in the Co(II)/PAA system. Conditions: [sulfa] = 50 mg L⁻¹, [PAA] = 800 μM, [Co²⁺] = 2 μM.

(30). Endowed with a terminal –O–OH group, PAA is recognized as a “PMS-like” oxidant. Therefore, the unwilling –NH₂-oxidation side reactions, which pose a universal challenge in oxidative wastewater treatment, might share a similar mechanism in these systems.

Although these azo by-products were expected to be removed by further oxidation processes (31), they exhibited relatively high stability in AOPs (32). A long-term monitoring shows that

the absorbance of by-products at 350 nm did not decrease throughout the reaction, and dosing more PAA could not remove these by-products (Fig. 3b). The reaction exhibited pseudo-zero-order kinetics during the initial stage, while the reaction rate gradually decreased with the consumption of reactants. The calculated kinetic constants were linearly related to the aniline and Co²⁺ concentrations (Fig. 3c and d). However, excess PAA did not substantially increase the kinetic constants, but instead

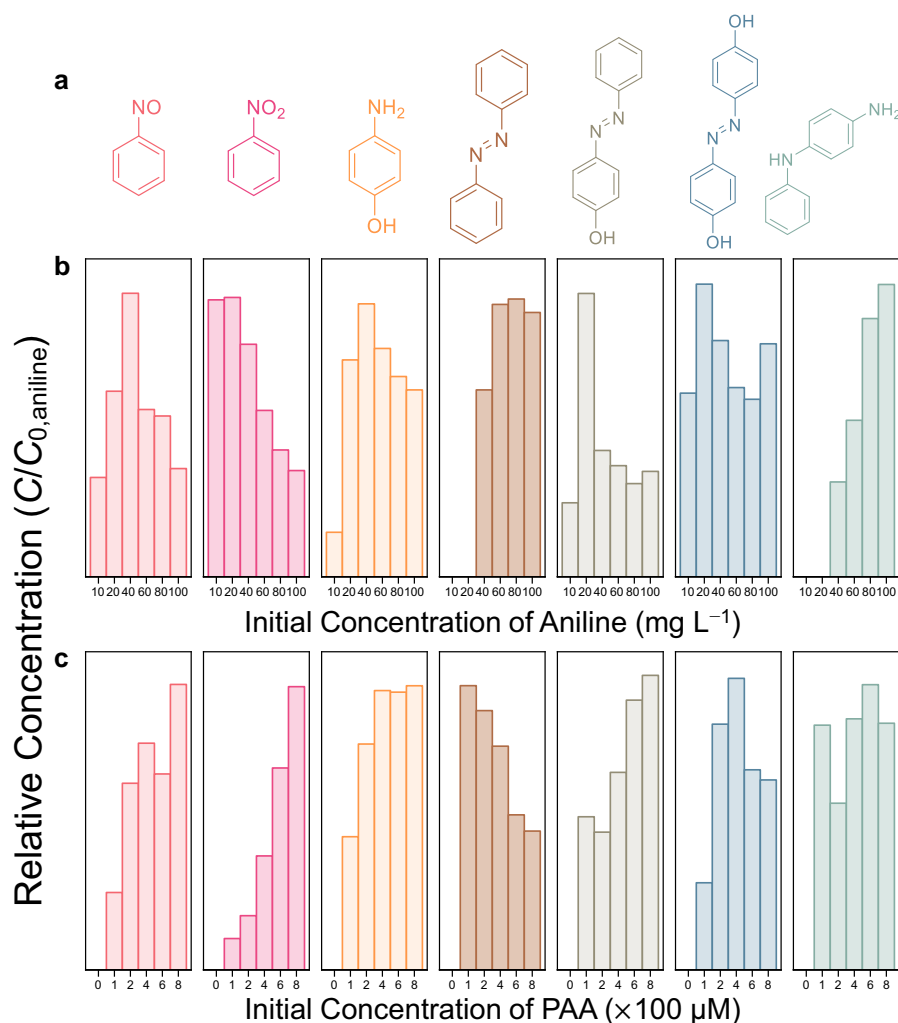


Fig. 2. Side reactions of aniline degradation in the Co(II)/PAA system. a) Identified intermediates and by-products of aniline degradation. b) Variations in the concentration of the identified products (relative to the initial concentration of aniline) at different initial aniline dosages. Conditions: [PAA] = 800 μM , $[\text{Co}^{2+}] = 2 \mu\text{M}$. c) Variation in the concentration of the identified products (relative to the initial concentration of aniline) at different dosages of PAA. Conditions: [aniline] = 100 mg L^{-1} , $[\text{Co}^{2+}] = 2 \mu\text{M}$.

prolonged the pseudo-zero-order stage (Fig. 3e). These results suggest that the rate-determining step of the reaction was between aniline and the reactive Co species.

Transformations of AAs in the Co(II)/PAA system

The possible transformation pathways of different AAs are summarized in Fig. 4. AAs with varying aromatic rings possess diverse bio- and medical-activities, depending on their distinct chemical structures. We found that the reactivity of $-\text{NH}_2$ increased with the electron density of the aromatic ring, leading to the formation of various by-products in the Co(II)/PAA system (Table S4). Such a reactive $-\text{NH}_2$ could also be substituted by $-\text{OH}$ and further transformed into a quinone. These by-products were found to be much more toxic than the original substances. However, in the presence of two $-\text{NH}_2$ on the naphthyl ring (2,3-diaminonaphthalene, DAN), most of the aforementioned by-products became unstable in the oxidation process. On the contrary, the formations of two totally $-\text{NH}_2$ -oxidized compounds could be observed, which were considerably stable in AOP systems but would be harmful to ecosystems. Similarly, the biphenyl ring of 4-aminobiphenyl enabled the coupling or oxidation of $-\text{NH}_2$ and promoted the hydroxylation

reactions that generated nitrosation, nitration, and coupling products with $-\text{OH}$ substitution.

In both natural and engineered systems, AAs with different heterocyclic aromatic rings are widely distributed and commonly detected. Heterocyclic atoms not only increase the reactivity of the $-\text{NH}_2$ but also decrease the stability of the aromatic rings. Hence, some ring-opening products were detected in the degradation of 2-aminobenzothiazole, which were evaluated to be harmless. Furthermore, nucleic acid-related AA produced no coupling by-products under oxidative stress, showing limited toxicity when treated with the Co(II)/PAA system.

AA-derived pharmaceuticals commonly contain deactivating groups. In noncatalytic processes, the reactions between PAA and various AAs have been well studied, and the deactivating groups were found to reduce the electron density on $-\text{NH}_2$ and inhibit its oxidation (33). Therefore, it is hypothesized that side reactions such as nitrosation, nitration, and coupling of $-\text{NH}_2$ are limited by the deactivating groups (34). However, this conclusion cannot be extrapolated to catalytic oxidation systems, because highly reactive species could readily reactivate the aromatic rings. The presence of strong deactivating groups, such as $-\text{NO}_2$, limited the direct coupling between the 4-nitroaniline (NOA) molecules

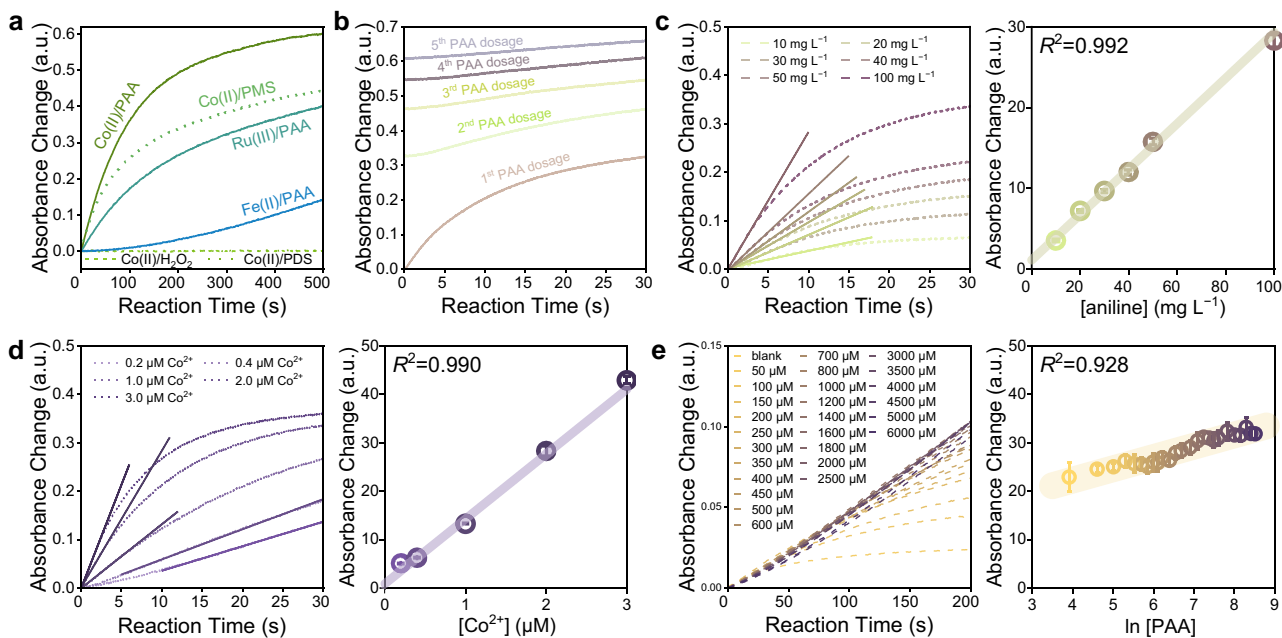


Fig. 3. Kinetic analysis of aniline in the Co(II)/PAA system. a) Comparison of the absorbance changing curves at 350 nm for the different catalytic oxidation systems. b) The kinetic absorbance at 350 nm after five repeated dosages of PAA. c) Effect of aniline dosage on the kinetics of by-product formation. Conditions: [PAA] = 800 μM , $[\text{Co}^{2+}] = 2 \mu\text{M}$. d) Effect of Co^{2+} concentration on the kinetics of by-product generation. Conditions: [PAA] = 800 μM , [aniline] = 100 $\text{mg}\cdot\text{L}^{-1}$. e) Effect of PAA dosage on the kinetics of by-product generation. Conditions: $[\text{Co}^{2+}] = 2 \mu\text{M}$, $[\text{Fe}^{2+}] = [\text{Ru}^{3+}] = 800 \mu\text{M}$, [aniline] = 100 $\text{mg}\cdot\text{L}^{-1}$.

(Table S5). In the Co(II)/PAA/NOA system, the hydroxylation activation of $-\text{NH}_2$ resulted in the formation of two extremely toxic by-products, **OA-NOA** and **OOA-NOA**. Also, substituting alkyl ($-\text{R}$) or alkoxy ($-\text{OR}$) groups could slightly increase the electron density on the aromatic rings, thereby altering the possible side reactions of the corresponding AAs. Among these side reactions, the coupling products were relatively toxic, while some nitrosation or nitration products might exhibit weaker toxicity than their parent compounds.

Acidic groups, such as $-\text{SO}_3\text{H}$, $-\text{COOH}$, and $-\text{AsO}_3\text{H}_2$, are usually classified as deactivating groups (35). However, their substitutions exhibited different effects on the side reactions of AAs. The presence of $-\text{SO}_3\text{H}$ and $-\text{COOH}$ significantly reduced the electron density on the benzene ring, thereby limiting the formation of by-products. Only after hydroxylation could sulfanilic acid and 2-aminoterephthalic acid be coupled with other hydroxylated substrates. Only azo products with two $-\text{OH}$ groups (i.e. **OOA**-products) were identified. In contrast, the electron-withdrawing effect of $-\text{AsO}_3\text{H}_2$ was weaker than these two groups and could undergo various side reactions. $-\text{AsO}_3\text{H}_2$ was a good leaving group under oxidative pressure, and nitrobenzene was also detected during the degradation of arsanilic acid (ASA), implying the generation of inorganic arsenic species. Generating toxic As(V) species in AOP systems might pose severe risks to water safety. Therefore, coupling-adsorption might be an efficient and safe strategy for ASA removal because the toxicity of coupling products did not significantly increase compared to ASA (36).

Halo groups are classified into deactivating groups, thus the degradation rates of AAs were slightly decreased after halogenations. However, halogenation could increase the electron density on the N atom of $-\text{NH}_2$ via the resonance effect. Consequently, although these reactions were slowed down, more complex side reactions occurred in the Co(II)/PAA process. The position of the halogen atoms affected the reaction performances of AAs due to

the different resonance effects (Table S7). These results support the hypothesis that the AOP-dominated hydroxylation step enhanced the reactivity of the $-\text{NH}_2$ group, leading to initiating coupling reactions via a nitrosation step. However, such an activation simultaneously decreased the reactivity of $-\text{NH}_2$ as a $-\text{NO}$ acceptor, resulting in the mono-hydroxylated azo products as the usually preferred coupling by-products.

AAs containing activating groups possess high electron densities on their aromatic rings, which led to the perception that they can be readily removed using AOP systems. As electron-donating groups, $-\text{CH}_3$ and $-\text{NH}_2$ increased the preference for hydroxylation and $-\text{OH}$ substitution. Consequently, azo and dimerization products with or without hydroxylation were commonly detected, and most of these by-products are more toxic than the parent compounds (Table S8). Notably, no ring-opening products were detected, suggesting that the toxic products of these AAs with activating groups were also stable and could accumulate in the Co(II)/PAA process.

The above results indicate that the estimated reactivity of AA with PAA may overlook the possibility of actual side reactions involving catalysts and reactive species in AOPs (34). Such catalytic systems might reactivate deactivated aromatic rings due to hydroxylation steps caused by oxidative reactive species. These findings suggest that the azo by-products involving AAs treatment could be prevalent in AOPs, and the associated risks should be fully evaluated.

Reactivity of AAs in the Co(II)/PAA system

The change profiles of AA concentrations were monitored by a concentration quantification method based on conventional chromatography, which exhibited pseudo-first-order kinetics (Fig. S2). The calculated kinetic constants were mainly determined by the energy of the highest occupied molecular orbital

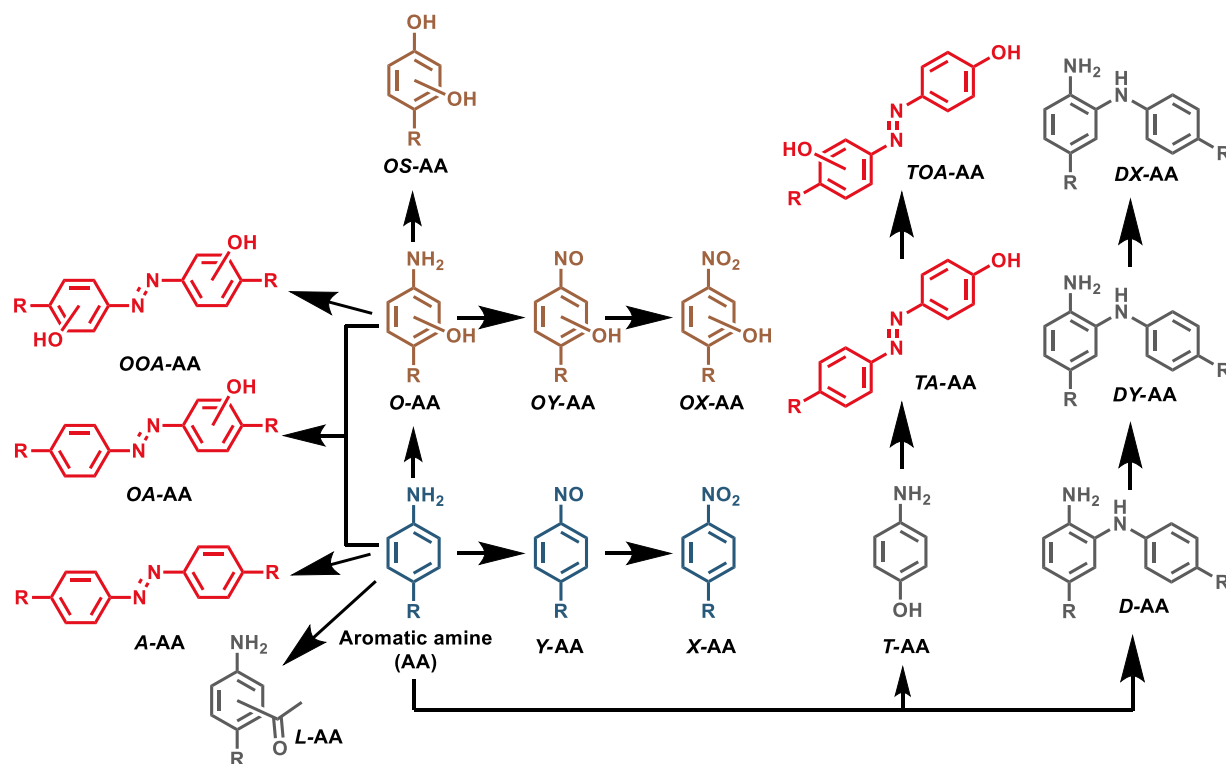


Fig. 4. Transformation pathways of different AAs in the Co(II)/PAA systems.

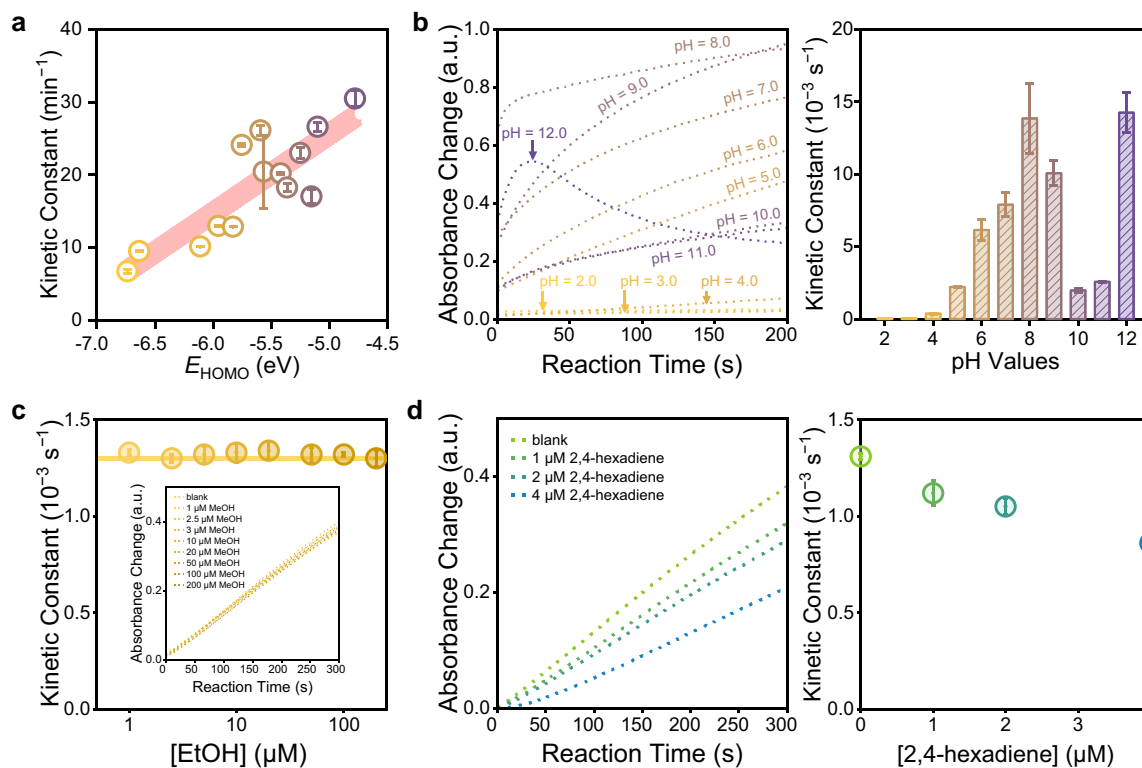


Fig. 5. a) The correlation between the measured kinetic constants and the calculated E_{HOMO} values. b) Effect of pH on the kinetics of by-product formation. Effect of c) MeOH (as a HO^\bullet quencher) and d) 2,4-hexadiene (as an R-O^\bullet quencher) on the kinetics of by-product generation. Conditions: $[\text{Co}^{2+}] = 2 \mu\text{M}$, $[\text{PAA}] = 800 \mu\text{M}$, $[\text{aniline}] = 100 \text{ mg L}^{-1}$.

(E_{HOMO}) of AAs (Fig. 5a), which is related to the electron transfer from aromatic compounds to highly oxidative species (10). This result indicates that the oxidative hydroxylation increased

the electron density of the amino $-\text{NH}_2$, initiating the subsequent $-\text{NH}_2$ oxidation and oxidative coupling reactions. Therefore, the side reactions of AAs in the PAA-activated systems would be

different from those in noncatalytic systems (34), and the generation of harmful by-products should be evaluated prior to their application in actual wastewater treatment.

In practical applications, pH can also significantly switch the generated oxidative active species, affecting the production of by-products. Thus, we also investigated the effect of pH on the reactivity of aniline coupling in the Co(II)/PAA system (Fig. 5b), which exhibited a complex trend. At low pHs (pH < 3.0), the generation of coupling products was completely inhibited. Under acidic conditions, the Co(II)/PAA system was unable to remove SMZ, indicating that oxidative species responsible for the $-\text{NH}_2$ coupling could not be produced (7). As the pH value was increased from 4.0 to 8.0, the efficiency of PAA activation by Co(II) increased, facilitating the aniline coupling. However, when the pH value was further increased to 11.0, the generation of coupling products decreased due to the self-catabolism of PAA ($pK_a = 8.2$), resulting in a low efficiency of Co(II)-catalyzed PAA decomposition. At pH 12.0, the coupling products were rapidly generated and consumed, implying that the precipitated $\text{Co}(\text{OH})_2$ might trigger different reactive species under alkaline conditions. It could not remove sulfonamides, but oxidized the aniline $-\text{NH}_2$.

Notably, the $-\text{NH}_2$ coupling reactions shared the active species in the Co(II)/PAA system responsible for pollutant removal. Thus, it could not be avoided by controlling the selectivity of reactive species generation. Moreover, the side reactions of aniline could occur over a wide pH range, exceeding the working pH range for sulfonamide removal by the Co(II)/PAA system. Thus, careful identification and toxicity assessment of the by-products are essential.

Catalytic mechanism for $-\text{NH}_2$ oxidation in the Co(II)/PAA system

To identify the reactive species responsible for the complex $-\text{NH}_2$ oxidation, we conducted quenching experiments in a kinetic spectroscopy study. Methanol (MeOH) was dosed to quench the possible $\cdot\text{OH}$, which showed a negligible effect on the kinetics of the generation of colored azo products (Fig. 5c). However, dosing 2,4-hexadiene resulted in a slight reduction in the generation of azo products (Fig. 5d), indicating that the oxidative organic radicals could not directly attack amino $-\text{NH}_2$ but were involved in forming dominant reactive species. Consequently, such side reactions could be mainly attributed to the oxidative Co species associated with the organic radicals formed after PAA activation (37). The Co-peroxide complexes (i.e. $\text{Co}-\text{OOSO}_3^-$ or $\text{Co}-\text{OOC}(\text{O})\text{CH}_3$) are frequently observed in Co(II)/peroxide systems using oxidants with an acidic terminal $-\text{OOH}$ group (38, 39). Such complexes also enabled a similar coupling behavior of aniline in the Co(II)/PMS system (Fig. 3a). The electrophilic Co-peroxide complexes could undergo single-electron-transfer reactions, leading to hydroxylation and $-\text{NH}_2$ coupling. Also, these complexes can directly cause $-\text{NH}_2$ oxidations via oxygen-atom-transfer reactions, including nitrosation and nitration.

Electron spin resonance (EPR) spin-trapping experiments were then conducted to investigate the behaviors of oxidative species within the Co(II)/PAA system. Initially, the generation of $^1\text{O}_2$ was evaluated in both the Co(II)/PAA and Co(II)/PMS systems (40), both of which exhibited the ability to induce $-\text{NH}_2$ oxidations (Fig. 3a). Dosing Co(II) into the PMS system led to an accelerated TEMPO accumulation, signifying efficient $^1\text{O}_2$ production. However, such a $^1\text{O}_2$ -induced TEMPO generation was absent in the Co(II)/PAA system (Fig. S3). Therefore, the Co(II)/PAA system presented an advantageous platform for unraveling the distinct

mechanism that underlied the unexpected $-\text{NH}_2$ oxidation, thereby eliminating the need to consider the role of $^1\text{O}_2$ in by-product formations. Besides, it was previously reported that 5,5-dimethyl-1-pyrroline-*N*-oxide (DMPO) could be directly oxidized to 5,5-dimethyl-2-pyrrolidone-*N*-oxyl (DMPOX) in the Co(II)/PAA system (39), which was also detected in our system (Fig. 6a). However, before the DMPOX accumulation, an adduct of DMPO with an O-centered radical was commonly detected, likely ascribed to the Co(II)-stabilized $\cdot\text{OOC}(\text{O})\text{CH}_3$ radical (i.e. $\text{Co}-\text{OOC}(\text{O})\text{CH}_3$ complex). Due to its inherent instability, it rapidly transformed into DMPOX but could be stabilized at high concentrations by MeOH (Fig. S3, $A_N = 14.4 \text{ G}$, $A_H = 11.0 \text{ G}$) (41).

To elucidate the mechanism behind the formation of DMPOX from the $\text{DMPO}-\text{OOC}(\text{O})\text{CH}_3$ adduct, we dosed a variety of quenching and chelating agents and also evaluated their effects on $-\text{NH}_2$ oxidation in the Co(II)/PAA/aniline system (Fig. 6a–c). Conventional radical quenchers, including MeOH, ethanol, isopropanol, tert-butanol (tBuOH), and dimethyl sulfoxide (DMSO), were found to efficiently scavenge the reactive radicals and inhibit the SMZ removal in the Co/PAA process (7, 39). However, these agents had no discernible effect on aniline coupling (Fig. 6c and d). PrOH and tBuOH inhibited the formation of DMPOX, suggesting enhanced stability of $\text{DMPO}-\text{OOC}(\text{O})\text{CH}_3$ adduct. Their presence also affected the degradation of SMZ. As shown in Fig. 6e, MeOH did not reduce SMZ removal in the Co(II)/PAA system, but increased the yield of by-products, suggesting that MeOH primarily modulated the selectivity between $-\text{NH}_2$ oxidation and C-centered attacks. Conversely, DMSO did not significantly change the by-product yield but reduced SMZ removal from 99.7 to 26.6%, highlighting its main function as an inhibitor of C-atom attacks with a negligible effect on $-\text{NH}_2$ oxidation. Moreover, Br^- was found to accelerate DMPOX generation, initially slowing down $-\text{NH}_2$ oxidation in the Co(II)/PAA/aniline system, and subsequently accelerating it. These results suggest the negligible generation of free radicals in the Co(II)/PAA system. Instead, all reactions, including DMPO transformation, $-\text{NH}_2$ oxidation, and the main-chain degradation of pollutants, are initiated by forming the $\text{Co}-\text{OOC}(\text{O})\text{CH}_3$ complex.

To prevent the formation of $\text{Co}-\text{OOC}(\text{O})\text{CH}_3$ complexes, we dosed ethylenediaminetetraacetate (EDTA) and tartrate chelating agents for Co species (42), effectively suppressing the generation of DMPOX (Fig. 6a). However, the amount of the DMPO adducts did not increase during the observation, and the AA degradations and the $-\text{NH}_2$ oxidation were significantly inhibited after dosing chelators. Therefore, the formation of DMPO adducts with O-centered residues in these systems may be ascribed to rapid direct oxidation by $[\text{Co}^{\text{III}}(\text{EDTA})]^-$ or $[\text{Co}^{\text{III}}(\text{tartrate})]^-$. Such a $\text{DMPO}-\text{OH}$ signal faded, while DMPOX was gradually formed after continuous oxidation. These results reveal that the $\text{Co}-\text{OOC}(\text{O})\text{CH}_3$ complex was an important active species for the rapid generation of DMPOX by first forming the $\text{DMPO}-\text{OOC}(\text{O})\text{CH}_3$ adduct as an intermediate. In addition, the $\text{Co}-\text{OOC}(\text{O})\text{CH}_3$ complex played a crucial role in the oxidation of AAs in the Co(II)/PAA system (Fig. 7). Notably, the unexpected $-\text{NH}_2$ oxidations are attributed to the high-valent Fe species (i.e. Fe^{IV}) in the ferrate oxidation process (43), suggesting that these deleterious side reactions and the corresponding mechanisms would not be specific to the Co(II)/PAA system (Fig. S1).

Conclusion

Transition metal/PAA processes have been widely studied because of their great potential in treating persistent organic

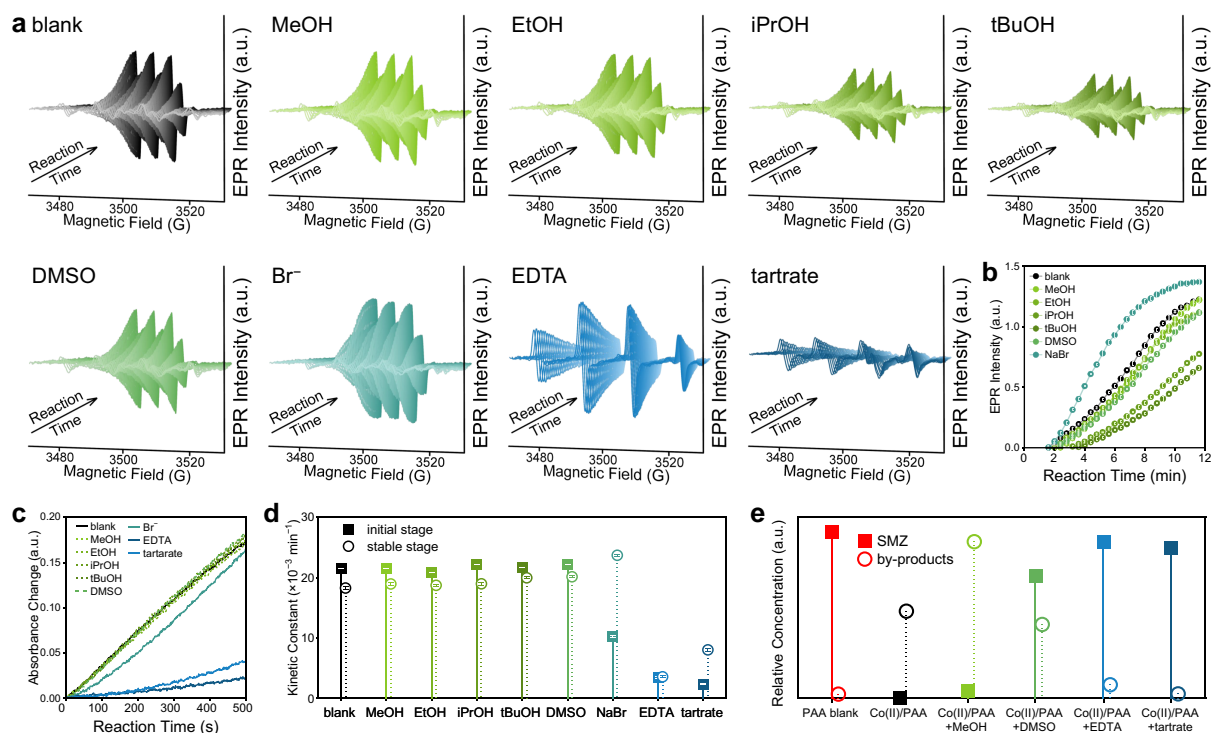


Fig. 6. a) Curves of EPR spectra in the different Co(II)/PAA systems. b) Measurements of EPR intensities of the DMPOX in these systems. c) Effects of quenchers and masking agents of Co^{2+} on the kinetics of by-product generation and (d) the corresponding kinetic constants. e) Effects of quenchers and masking agents of Co^{2+} on the SMZ degradation and side reactions. Conditions: $[\text{DMPO}] = 100 \text{ mM}$, $[\text{Co}^{2+}] = 2 \text{ }\mu\text{M}$, $[\text{PAA}] = 800 \text{ }\mu\text{M}$, $[\text{aniline}] = 100 \text{ mg L}^{-1}$, $[\text{SMZ}] = 10 \text{ }\mu\text{M}$, $[\text{quencher}] = [\text{masking agent}] = 1 \text{ mM}$.

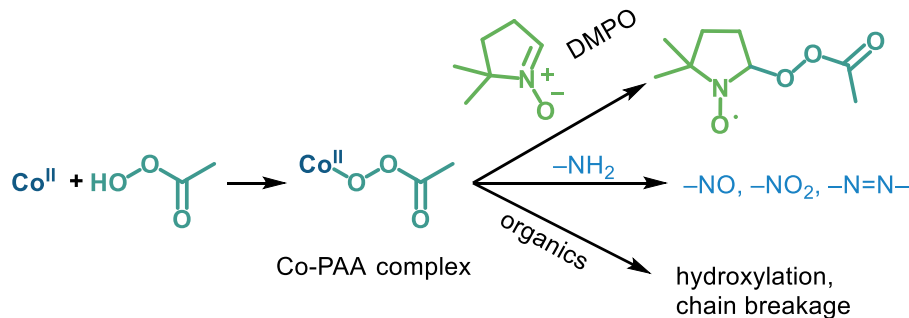


Fig. 7. A schematic illustration showing the formation of the Co-peroxide complex and its interaction with $-\text{NH}_2$.

pollutants, such as sulfa drugs. However, evaluating the effectiveness of these processes for contaminant degradation is complicated by the presence of acetate residues. In this work, we found that in a model Co(II)/PAA system, the $-\text{NH}_2$ moieties were unexpectedly oxidized to form $-\text{NO}$, $-\text{NO}_2$, and $-\text{N}=\text{N}-$ moieties. We identified the highly oxidative $\text{Co}-\text{OOC}(\text{O})\text{CH}_3$ complex as the reactive species responsible for the unexpected oxidation of aromatic $-\text{NH}_2$. This complex could activate the aromatic $-\text{NH}_2$ moieties, thus causing their harmful oxidations to be prohibitive in noncatalytic systems. By varying the structures of targeted AA compounds, we revealed the complex side reactions of AAs in this model AOP system. Our findings indicate that the most stable by-products produced in the Co(II)/PAA system were persistent. The predicted toxicities of these long-lasting by-products reveal the risks of using this AOP system to treat AA-containing wastewater. Moreover, the oxidative hydroxylation increased the toxicity of the resulting by-products. Thus, developing a safe and effective method to treat AA-containing wastewater is a

challenge. The results from this work enhance our understanding about the complexities of AA treatment and will contribute to developing more efficient and toxic by-product-free wastewater treatment processes. Also, such an approach would be adaptively extended to more complex systems. With slight modifications, it could also serve as a useful paradigm in nonchemically catalyzed systems such as UV/PAA systems.

Materials and methods

Materials

All reagents used in this work were purchased from Aladdin Reagent Co., China, and no further purification was required unless stated otherwise. The properties of aromatic amines used in this work are summarized in Table S1. To denote the complex intermediate and by-products generated in the Co(II)/PAA system, we used different symbols to represent possible reactions

Table 1. Symbols for different reactions of target pollutants.

Reaction	Symbol	Reaction	Symbol
Nitrosation	Y	Hydroxylation	O
Nitration	X	Ring opening	R
Coupling	A	Chain breakage	C
Substitution of $-NH_2$	S	Substitution of other moieties	T
Dimerization	D	Acetylation	L

(Table 1). The designation of a product was composed of the reaction symbols and the abbreviation of the parent compound.

Experimental procedures

All experiments were conducted at ambient temperature. Kinetics studies were carried out in a glass reactor (100 mL) with continuous magnetic stirring (450 rpm). In the reactor, the predetermined amount of $Co(CH_3COO)_2$ was dispersed into 50 mL of the appropriate concentration of contaminant solution, and the experiments started when a predetermined concentration of PAA solution (1 mL) was injected into the suspension. For the by-product analysis, samples were collected without quenching. For kinetic analysis, samples of 1 mL were taken at given time intervals and quenched with excess sodium thiosulfate ($Na_2S_2O_3$, 20 mM).

Analytical methods

The intermediates in the $Co(II)/PAA$ system were analyzed by a liquid chromatography coupled with a mass spectrometer (LC–MS, AB Triple TOF 5600+, AB Sciex, USA) for detection and an Xbridge BEH C18 column (2.5 μm , 2.1 mm \times 100 mm, Waters Inc., USA) was used. The eluent consisted of acetonitrile (eluent A) and 0.1% formic acid in water (eluent B) at a flow rate of 0.3 mL min^{-1} . The gradient program for the volume ratios was as follows: 0–3 min, 95% A; 3–8 min, 95–50% A; 8–10 min, 50% A; 10–11 min, 50–5% A; 11–17 min, 5% A; 17–18 min, 5–95% A; 18–20 min, 95% A. A scan range of m/z 50–600 was selected in both positive and negative modes.

The UV–Vis spectra of the aqueous $Co(II)/PAA/AAs$ systems were acquired using a scanning spectrophotometer (Lambda 650s, PerkinElmer Inc., USA). To monitor the generation of azo products in aniline degradation, the in situ kinetic spectra were acquired at 350 nm.

EPR spectra for detecting reactive species

DMPO was used as a radical trapper. The spectra were acquired by an EPR spectrometer (EMX Plus, Bruker Co., Germany). The modulation amplitude, microwave power, and microwave frequency were set at 2.0 G, 2.0 mW, and 9.8422 GHz, respectively. In a typical EPR measurement, the different $Co(II)/PAA$ systems and the spin trapper were mixed into a glass capillary and immediately inserted into the lumen of EPR spectrometer. All scans were performed at ambient temperature with the following EPR instrument settings: sweep width, 120 G; power, 2.0 mW; modulation amplitude, 2.0 G; time constant, 10.24 ms; conversion time, 6.94 ms; sweep time, 24.98 s. The spectra were continuously acquired without delay (40).

Acknowledgments

The authors thank Ms. Haiyan Zhang at University of Science and Technology of China for helping with the LC–MS analysis.

Supplementary Material

Supplementary material is available at PNAS Nexus online.

Funding

The authors thank the National Natural Science Foundation of China (51821006, 52192684, 52027815, and 52270149) for supporting this work. J.-H.W. acknowledges the financial support from the Shanghai Tongji Gao Tingyao Environmental Science & Technology Development Foundation, China.

Author Contributions

H.-Q.Y., F.C., J.-H.W., and T.-H.Y. conceived and planned the experiments and carried out the relative experiments. J.-H.W. and F.C. analyzed various characterizations. H.-Q.Y. contributed to the planning and coordination of the project. J.-H.W. wrote the initial draft of the manuscript and further modified by F.C. and H.-Q.Y. All authors contributed to the discussion of the results and the manuscript.

Data Availability

All data are included in the article and Supplementary material.

References

- Nishizawa A, et al. 2019. Nickel-catalyzed decarboxylation of aryl carbamates for converting phenols into aromatic amines. *J Am Chem Soc.* 141:7261–7265.
- Migliorini F, et al. 2023. Switching mechanistic pathways by micellar catalysis: a highly selective rhodium catalyst for the hydroaminomethylation of olefins with anilines in water. *ACS Catal.* 13:2702–2714.
- Muz M, Krauss M, Kutsarova S, Schulze T, Brack W. 2017. Mutagenicity in surface waters: synergistic effects of carboline alkaloids and aromatic amines. *Environ Sci Technol.* 51:1830–1839.
- Shi H, He Y, Li Y, Luo P. 2023. Unraveling the synergy mechanism between photocatalysis and peroxymonosulfate activation on a Co/Fe bimetal-doped carbon nitride. *ACS Catal.* 13:8973–8986.
- Sági G, et al. 2018. Radiolysis of sulfonamide antibiotics in aqueous solution: degradation efficiency and assessment of antibacterial activity, toxicity and biodegradability of products. *Sci Total Environ.* 622–623:1009–1015.
- Du J, et al. 2020. Periodate activation with manganese oxides for sulfanilamide degradation. *Water Res.* 169:115278.
- Wang Z, et al. 2020. Application of cobalt/peracetic acid to degrade sulfamethoxazole at neutral condition: efficiency and mechanisms. *Environ Sci Technol.* 54:464–475.
- Wang J, et al. 2020. Thermal activation of peracetic acid in aquatic solution: the mechanism and application to degrade sulfamethoxazole. *Environ Sci Technol.* 54:14635–14645.
- Li R, et al. 2021. Peracetic acid–ruthenium(III) oxidation process for the degradation of micropollutants in water. *Environ Sci Technol.* 55:9150–9160.
- Kim J, et al. 2020. Cobalt/peracetic acid: advanced oxidation of aromatic organic compounds by acetylperoxyl radicals. *Environ Sci Technol.* 54:5268–5278.
- Kiejza D, Kotowska U, Polińska W, Karpińska J. 2021. Peracids—new oxidants in advanced oxidation processes: the use of peracetic acid, peroxymonosulfate, and persulfate salts in the removal

- of organic micropollutants of emerging concern—a review. *Sci Total Environ.* 790:148195.
- 12 Moreno-Andrés J, et al. 2023. Evaluation of algacide effectiveness of five different oxidants applied on harmful phytoplankton. *J Hazard Mater.* 452:131279.
- 13 Cai S, et al. 2013. Room temperature activation of oxygen by monodispersed metal nanoparticles: oxidative dehydrogenative coupling of anilines for azobenzene syntheses. *ACS Catal.* 3: 478–486.
- 14 Jakubczyk M, et al. 2022. Mechanochemical conversion of aromatic amines to aryl trifluoromethyl ethers. *J Am Chem Soc.* 144:10438–10445.
- 15 Chen C, et al. 2021. Formation of nitro(so) and chlorinated products and toxicity alteration during the UV/monochloramine treatment of phenol. *Water Res.* 194:116914.
- 16 Brown MA, De Vito SC. 1993. Predicting azo dye toxicity. *Crit Rev Environ Sci Technol.* 23:249–324.
- 17 Kong Z, Li L, Xue Y, Yang M, Li Y-Y. 2019. Challenges and prospects for the anaerobic treatment of chemical-industrial organic wastewater: a review. *J Clean Prod.* 231:913–927.
- 18 Yan Y, et al. 2021. Synthesis of Fe⁰/Fe₃O₄@porous carbon through a facile heat treatment of iron-containing candle soots for peroxymonosulfate activation and efficient degradation of sulfamethoxazole. *J Hazard Mater.* 411:124952.
- 19 Zhu J, Chen C, Li Y, Zhou L, Lan Y. 2019. Rapid degradation of aniline by peroxydisulfate activated with copper-nickel binary oxy-sulfide. *Sep Purif Technol.* 209:1007–1015.
- 20 Yang Y, et al. 2017. Degradation of sulfamethoxazole by UV, UV/H₂O₂ and UV/persulfate (PDS): formation of oxidation products and effect of bicarbonate. *Water Res.* 118:196–207.
- 21 Yu Y, Ji Y, Lu J, Yin X, Zhou Q. 2021. Degradation of sulfamethoxazole by Co₃O₄-palygorskite composites activated peroxymonosulfate oxidation. *Chem Eng J.* 406:126759.
- 22 Ra J, Yoom H, Son H, Hwang T-M, Lee Y. 2019. Transformation of an amine moiety of atenolol during water treatment with chlorine/UV: reaction kinetics, products, and mechanisms. *Environ Sci Technol.* 53:7653–7662.
- 23 Wu W, et al. 2020. Degradation of organic compounds by peracetic acid activated with Co₃O₄: a novel advanced oxidation process and organic radical contribution. *Chem Eng J.* 394:124938.
- 24 Wang J, et al. 2021. Applying a novel advanced oxidation process of activated peracetic acid by CoFe₂O₄ to efficiently degrade sulfamethoxazole. *Appl Catal B.* 280:119422.
- 25 Wang J, et al. 2021. Molybdenum disulfide (MoS₂): a novel activator of peracetic acid for the degradation of sulfonamide antibiotics. *Water Res.* 201:117291.
- 26 Xiong J-Q, et al. 2020. Insights into the effect of cerium oxide nanoparticle on microalgal degradation of sulfonamides. *Bioresour Technol.* 309:123452.
- 27 An Z, et al. 2021. Full insights into the roles of pH on hydroxylation of aromatic acids/bases and toxicity evaluation. *Water Res.* 190:116689.
- 28 Qiao J, Jiao W, Liu Y. 2021. Degradation of nitrobenzene-containing wastewater by sequential nanoscale zero valent iron-persulfate process. *Green Energy Environ.* 6:910–919.
- 29 Gadaleta D, Manganelli S, Manganaro A, Porta N, Benfenati E. 2016. A knowledge-based expert rule system for predicting mutagenicity (Ames test) of aromatic amines and azo compounds. *Toxicology.* 370:20–30.
- 30 Zong Y, et al. 2020. Unraveling the overlooked involvement of high-valent cobalt-oxo species generated from the cobalt(II)-activated peroxymonosulfate process. *Environ Sci Technol.* 54:16231–16239.
- 31 Zhang T, Huang CH. 2020. Modeling the kinetics of UV/peracetic acid advanced oxidation process. *Environ Sci Technol.* 54: 7579–7590.
- 32 Muthukumar M, Sargunamani D, Selvakumar N. 2005. Statistical analysis of the effect of aromatic, azo and sulphonic acid groups on decolouration of acid dye effluents using advanced oxidation processes. *Dyes Pigm.* 65:151–158.
- 33 Ibne-Rasa KM, Edwards JO. 1962. The mechanism of the oxidation of some aromatic amines by peroxyacetic acid. *J Am Chem Soc.* 84:763–768.
- 34 Kim J, Huang CH. 2020. Reactivity of peracetic acid with organic compounds: a critical review. *ACS ES&T Water.* 1:15–33.
- 35 McMurry J. 2015. Chemistry of benzene: electrophilic aromatic substitution. In: *Organic chemistry*. 9th ed. United States of America: Cengage Learning. p. 493–503.
- 36 Ke M-K, et al. 2021. Interface-promoted direct oxidation of p-arsanilic acid and removal of total arsenic by the coupling of peroxymonosulfate and Mn-Fe-mixed oxide. *Environ Sci Technol.* 55:7063–7071.
- 37 Liu B, et al. 2021. Insights into the oxidation of organic contaminants by Co(II) activated peracetic acid: the overlooked role of high-valent cobalt-oxo species. *Water Res.* 201:117313.
- 38 Li H, Zhao Z, Qian J, Pan B. 2021. Are free radicals the primary reactive species in Co(II)-mediated activation of peroxymonosulfate? New evidence for the role of the Co(II)-peroxymonosulfate complex. *Environ Sci Technol.* 55:6397–6406.
- 39 Zhao Z, Li X, Li H, Qian J, Pan B. 2021. New insights into the activation of peracetic acid by Co(II): role of Co(II)-peracetic acid complex as the dominant intermediate oxidant. *ACS EST Engg.* 1:1432–1440.
- 40 Wu J-H, Chen F, Yang T-H, Yu H-Q. 2023. Unveiling singlet oxygen spin trapping in catalytic oxidation processes using in situ kinetic EPR analysis. *Proc Natl Acad Sci U S A.* 120:e2305706120.
- 41 Chen L, et al. 2022. Accurate identification of radicals by in situ electron paramagnetic resonance in ultraviolet-based homogeneous advanced oxidation processes. *Water Res.* 221:118747.
- 42 Folkman SJ, Soriano-Lopez J, Galán-Mascarós JR, Finke RG. 2018. Electrochemically driven water-oxidation catalysis beginning with six exemplary cobalt polyoxometalates: is it molecular, homogeneous catalysis or electrode-bound, heterogeneous CoO_x catalysis? *J Am Chem Soc.* 140:12040–12055.
- 43 Johnson MD, Hornstein BJ. 1996. Unexpected selectivity in the oxidation of arylamines with ferrate—preliminary mechanistic considerations. *Chem Commun.* 8:965–966.